ON FINITE PLASTIC FLOWS OF COMPRESSIBLE MATERIALS WITH INTERNAL FRICTION

S. NEMAT-NASSER

Departments of Civil Engineering and Applied Mathematics, Northwestern University, Evanston, IL 60201, U.S.A.

and

A. SHOKOOH

Department of Civil Engineering, Northwestern University, Evanston, IL 60201, U.S.A.

Abstract—For finite plastic deformations of porous metals and geotechnical materials such as cohesionless or cohesive soils, a theory is developed which accounts for plastic volumetric changes, pressure sensitivity, and microscopic frictional effects, and therefore involves a nonassociative flow rule. This development is based on a systematic modification of the usual J_2-flow potential and yield function. It is shown that a number of specialized, recently developed plasticity theories are special cases of the theory presented here. For illustration, the problem of triaxial testing of cohesionless sands or cohesive soils is analyzed in detail, and it is shown that the theory gives many of the experimentally observed responses of this kind of materials under monotone loading conditions. Finally, the simple shear test is examined, and possible application of the theory to stable and unstable fault motions, is mentioned.

1. INTRODUCTION

This paper develops a theory of work-hardening, finite-strain plasticity which may have direct application to dilatant materials in general, and to porous metals, rocks and granular materials such as sands and soils, in particular. It is known that the mechanical responses of materials of this kind are pressure sensitive, and that, due to changes in porosity and the presence of internal frictional and other effects, the usual incompressible theory of plasticity with normality and associated flow rule does not apply. Moreover, both for grandular materials and for ductile metals containing microvoids, large inelastic strains are encountered. Therefore, a systematic development of a plasticity theory for finite strains and including nonassociative flow rule and dilatancy (or compressibility) effect seems in order.

The present work unifies in a general context a number of specialized small-strain or finite-strain theories which have recently been considered by a number of writers in various contexts, see, e.g. Berg[1], Rudnicki and Rice[2] and Wilde[3]. Berg's[1] work pertains to (small) plastic deformation of microporous metal aggregates, and involves a pressure sensitive yield condition. Rudnicki and Rice[2] consider the formation of shear bands in rock masses, and develop a plasticity theory with nonassociative flow rule for finite strains. They introduce two constants, a dilantancy factor and an internal friction coefficient. They then generalize their formulation in an effort to account for the vertex-like structure of the yield surface, this generalization essentially amounting to the modification of the elastic and the work-hardening moduli. Wilde[3] proposes a small strain plasticity theory with normality and associative flow rule, based on the extension of the usual J_2-plasticity theory. He applies this theory to examine the mechanical behavior of granular materials in the context of the critical state soil mechanics; see Schofield and Wroth[4]. As we shall show, for dilatant materials with internal friction, the use of the associative flow rule leads to contradiction.

The theory presented here is a systematic extension of the usual J_2 theory of plasticity for finite strains and with nonassociative flow rule. Although there are some similarities between our work and the work of Wilde[3], our results go beyond the limited scope considered by Wilde, and avoids some essential inconsistancies that exist in Wilde's theory. For example, in our theory the dilatancy parameter relates directly to the flow potential, and is distinct from the internal frictional factor which relates to the yield function. Moreover, for soils in a triaxial state of stress, we obtain a relation between the dilatancy factor and the frictional coefficient

(both may be functions of pressure as well as plastic volume change), which provides us with a natural definition of the critical state as a consequence of the basic theory.

Our development follows the basic procedure of Hill[5]. In Section 2 the basic constitutive relations are developed in terms of the quantities common in continuum mechanics. A discussion of the results and a comparison with other theories are presented in Section 3. In Section 4 we apply the theory to a soil sample in triaxial stress state, and show how the theory includes as a special case all essential features contained in the critical state soil mechanics of Schofield and Wroth[4], our development, however, clearly shows that the use of an associative flow rule is in contradiction with the other assumptions of the critical state theory. In an effort to provide an easy comparison, in Section 4 we shall use notation common in soil mechanics.

2. FORMULATION OF THEORY

For simplicity, a fixed rectangular Cartesian coordinate system with coordinate axes, x_i, $i = 1, 2, 3$, is used. The material is regarded rate-independent, and therefore the time parameter may be any convenient monotone quantity; this parameter will be denoted by θ, and superimposed dot will designate material rate of change with respect to θ. With v_i designating the velocity field, and $D_{ij} = (1/2)(v_{i,j} + v_{j,i})$ standing for the deformation rate tensor, where comma followed by an index represents partial differentiation with respect to the corresponding coordinate, one has the following exact decomposition,[†] Hill[6]:

$$D_{ij} = D_{ij}^e + D_{ij}^p, \tag{2.1}$$

where superscript e stands for the elastic part, and superscript p for the plastic part. For problems of interest here, the elastic strain rate may be related to a (properly invariant) stress-rate by means of a linear relation similar to Hook's law. For example, with $\overset{*}{\sigma}_{ij}$ denoting the Jaumann rate of change of the Cauchy stress, σ_{ij},

$$\overset{*}{\sigma}_{ij} = \dot{\sigma}_{ij} - W_{ik}\sigma_{kj} - W_{jk}\sigma_{ki}, \quad i, j, k = 1, 2, 3, \tag{2.2}$$

we may set

$$D_{ij}^{e\prime} = \overset{*}{\sigma}_{ij}'/2\mu, \quad D_{kk}^e = \overset{*}{\sigma}_{kk}/3\kappa, \tag{2.3}$$

where repeated indices are summed, prime denotes the deviatoric part, μ is the elastic shear modulus, and κ is the elastic bulk modulus; in (2.2), $W_{ij} = (1/2)(v_{i,j} - v_{j,i})$ is the spin tensor.

The plastic part of the deformation rate tensor is expressed in terms of a flow potential, g, as[‡]

$$D_{ij}^p = \dot{\lambda} \frac{\partial g}{\partial \sigma_{ij}}, \tag{2.4}$$

where σ_{ij} is the total stress (the deviatoric part *plus* the spherical part), $\dot{\lambda}$ is a scalar function, and the flow potential g is assumed to depend on the state of stress including the hydrostatic pressure (or tension), on the total *plastic* volumetric strain, Δ, measured with respect to a suitable reference state, and on the total distortional plastic work, ξ, in the following manner:

$$g\sqrt{J} + G(I, \Delta, \xi), \tag{2.5}$$

[†]Unlike the deformation rate tensor, strains in finite deformations do not admit simple additive decomposition of the form (2.1). For a critical discussion of this and related points, see Nemat-Nasser[7].

[‡]Note that because of this, the orientation of the plastic strain rate, D_{ij}^p, is *not* affected by the orientation of the stress-rates $\overset{*}{\sigma}_{ij}$, however, one may include corners in the flow potential and the yield function.

where

$$J = \frac{1}{2}\sigma'_{ij}\sigma'_{ij}, \quad I = \sigma_{ii},$$

$$\Delta = \int_0^{\theta} \frac{\rho_0}{\rho} D^p_{ii}\, d\theta', \quad \xi = \int_0^{\theta} \frac{\rho_0}{\rho}\sigma'_{ij}D^p_{ij}\, d\theta'; \tag{2.6}$$

for simplicity in notation, we use J for the commonly used J_2, I for the commonly used I_1, and do not use superscript p on Δ, although it only represents the plastic part of the volumetric strain. In (2.6), ρ_0 and ρ are the mass density in the reference and in the current states, respectively. Later on we shall find it convenient to use the current configuration for reference. Then one sets $\rho_0 = \rho$ *after* the integration in (2.6)$_{3,4}$ is performed. Note that in accumulating the plastic volumetric change and the plastic distortional work, it is essential to use a common fixed reference configuration, especially since large volumetric changes may be involved. In (2.6), therefore, ξ and Δ represent, respectively, the distortional plastic work and the plastic volumetric change, both measured per unit volume in the reference configuration.

In addition to the flow potential, a yield function, f, in the following form is considered:

$$f = \sqrt{J} - F(I, \Delta, \xi). \tag{2.7}$$

Then the scalar parameter λ in (2.4) is determined from the consistency condition, $\dot{f} = 0$, and this yields,

$$\dot{\lambda} = \left(\sqrt{\dot{J}} - \frac{\partial F}{\partial I}\dot{I}\right)\Big/ H, \tag{2.8}$$

where

$$H = \frac{\rho_0}{\rho}\left(3\frac{\partial G}{\partial I}\frac{\partial F}{\partial \Delta} + \sqrt{J}\frac{\partial F}{\partial \xi}\right). \tag{2.9}$$

Since† $\sqrt{\dot{J}} = (1/2)\sigma'_{ij}\overset{*}{\sigma}_{ij}/\sqrt{J}$, and $\dot{I} = \overset{*}{\sigma}_{ii}$, (2.4) and (2.8) yield,

$$D^{p'}_{ij} = \frac{\sigma'_{ij}}{2H\sqrt{J}}\left(\frac{1}{2\sqrt{J}}\sigma'_{kl}\overset{*}{\sigma}_{kl} - \frac{\partial F}{\partial I}\overset{*}{\sigma}_{kk}\right), \tag{2.10}$$

$$D^p_{kk} = \frac{3}{H}\frac{\partial G}{\partial I}\left(\frac{1}{2\sqrt{J}}\sigma'_{kl}\overset{*}{\sigma}_{kl} - \frac{\partial F}{\partial I}\overset{*}{\sigma}_{kk}\right). \tag{2.11}$$

These equations hold as long as the yield condition, $f = \sqrt{J} - F = 0$, is satisfied.

From (2.9)–(2.11) it is seen that, as far as the flow potential g is concerned, only $\partial G/\partial I$ enters into the final constitutive relations. If both sides of (2.10) are multiplied by σ'_{ij}, the result summed on i and j, and (2.11) is used, one obtains,

$$3\frac{\partial G}{\partial I} = \frac{\sqrt{J}D^p_{kk}}{\sigma'_{ij}D^p_{ij}}. \tag{2.12}$$

Since the denominator in the right-hand side is positive, the left-hand side will have the same sign as D^p_{kk}. Hence, $3\partial G/\partial I$ is a measure of the instantaneous rate of plastic volumetric changes. Following the terminology of Rudnicki and Rice[2] and Mehrabadi and Cowin[8], we shall refer to $3\partial G/\partial I$ as the dilatancy factor. We note, however, that this factor is, in general, a function of I, Δ and ξ. It is possible in certain specific applications to express the dilatancy factor in terms of $\partial F/\partial I$. An example of this kind is worked out in Section 4. In general,

†Here only the Jaumann rate can be used in the form indicated.

however, one may treat the dilatancy factor as an independent constitutive parameter which may be positive, negative or zero, for the same material under different deformation and loading histories.

The quantity $\partial F/\partial I$ represents the sensitivity of material hardening to hydrostatic tension. In this sense it represents the effect of internal friction on yielding of granular materials.

Equations (2.10) and (2.11) are in form similar to eqns (10) of Rudnicki and Rice[2]. In fact, if the functions F and G are restricted so that $-\partial F/\partial I = \bar{\mu}/3$, and $\partial G/\partial I = \beta/3$, with $\bar{\mu}$ and β constants, and if H is identified with h, we obtain eqns (10) of [2], $\bar{\mu}$ here is not the shear modulus used before, but rather it is an internal frictional coefficient, and β is a dilatancy factor. Since the functions F and G can be suitably adjusted for specific applications, the present generalization seems to provide considerable flexibility. In general, for granular materials the effective friction and the instantaneous dilatancy are highly affected by the inelastic volumetric changes that have taken place, and by the corresponding inelastic distortions; the former appear to be more significant in cohesionless soils, whereas the latter play a dominant role in cohesive soils, such as clays—moreover, both materials are highly pressure sensitive. Similar comments may apply to rock masses, where microcracks, fissures, and joints exist, and their configuration and density change in the course of inelastic deformations. Equations (2.10) and (2.11) reflect these facts to a certain extent. In particular, it is noted that both the distortional and the dilatational parts of the deformation rate tensor can be made to depend on pressure, volumetric plastic strain, and the total distortional work; these and related aspects are more fully discussed later on.

If $\partial G/\partial I \equiv 0$, then $D_{kk}^p \equiv 0$ and from (2.6)$_3$ it follows that $\Delta = 0$. In this case, the material may be pressure sensitive only through the dependence of the yield function on the pressure, although it is plastically incompressible. When both $\partial G/\partial I$ and $\partial F/\partial I$ are identically zero, then one arrives at the Prandtle–Reuss plasticity equations.

Finally, one may combine the plastic and elastic deformation rates from (2.10), (2.11) and (2.3), into (2.1), and arrive at

$$D_{ij} = L_{ijkl}\overset{*}{\sigma}_{kl},$$ (2.13)

where

$$L_{ijkl} = \frac{1}{4\mu}(\delta_{ik}\delta_{jl} + \delta_{jk}\delta_{il}) + \left(\frac{1}{9\kappa} - \frac{1}{6\mu}\right)\delta_{ij}\delta_{kl}$$
$$+ \frac{1}{H}\left(\frac{\sigma'_{ij}}{2\sqrt{J}} + \frac{\partial G}{\partial I}\delta_{ij}\right)\left(\frac{\sigma'_{kl}}{2\sqrt{J}} - \frac{\partial F}{\partial I}\delta_{kl}\right).$$ (2.14)

The inverse of (2.13) is

$$\overset{*}{\sigma}_{ij} = M_{ijkl}D_{kl},$$ (2.15)

where

$$M_{ijkl} = \mu(\delta_{ki}\delta_{lj} + \delta_{kj}\delta_{li}) + \left(\kappa - \frac{2}{3}\mu\right)\delta_{ij}\delta_{kl} - \left(H + \mu - 9\kappa\frac{\partial F}{\partial I}\frac{\partial G}{\partial I}\right)^{-1}\left(\frac{\mu}{\sqrt{J}}\sigma'_{ij}\right.$$
$$\left. + 3\kappa\frac{\partial G}{\partial I}\delta_{ij}\right)\left(\frac{\mu}{\sqrt{J}}\sigma'_{kl} - 3\kappa\frac{\partial F}{\partial I}\delta_{kl}\right).$$ (2.16)

Equations (2.13)–(2.16) provide a complete set of constitutive relations for plastic materials whose response involves plastic volume changes, large plastic deformations, and that do not comply with the usual assumptions of normality and associative flow rule. In the following section these equations are contrasted to equations proposed by Rudnicki and Rice[2] and by Wilde[3], and an alternative formulation in terms of the effective plastic strain is given.

3. DISCUSSION AND COMPARISON WITH OTHER RESULTS

If one introduces the "effective" shear stress and the "effective" shear strain increment as

$$\bar{\tau} = \sqrt{J}, \quad d\bar{\gamma} = (2D_{ij}^{p'} D_{ij}^{p'})^{1/2} \, d\theta, \tag{3.1}$$

then in a simple shear test the tangent to the shear stress-plastic shear strain curve is given by $h = d\bar{\tau}/d\bar{\gamma}$. For proportional loading and when $\rho_0 \approx \rho$, it can be shown (Hill[5]) that $\sqrt{J}\partial F/\partial\xi$ in eqn (2.9) equals the tangent modulus h. Hence, in a general case we may follow the usual practice and define

$$h = \frac{\rho_0}{\rho} \sqrt{J} \frac{\partial F}{\partial \xi}. \tag{3.2}$$

Then the work-hardening parameter, H, may be expressed as[†]

$$H = h_1 + h, \tag{3.3}$$

where

$$h_1 = 3 \frac{\rho_0}{\rho} \frac{\partial G}{\partial I} \frac{\partial F}{\partial \Delta}. \tag{3.4}$$

The quantity h measures work-hardening induced by plastic distortion, whereas h_1 corresponds to hardening (or softening) due to volumetric and pressure effects. For this reason one may refer to h_1 as "density-hardening" parameter. For loose sands, e.g. only the density-hardening parameter seems to be of importance. We observe that when $h = 0$, then $\partial G/\partial I = 0$ implies $H = 0$ and $D_{kk}^p = 0$. Moreover, granular materials harden as they compact and soften as they dilate. Then if one regards compression and compaction positive (tension and dilation negative), i.e. $\Delta > 0$ for volume decrease, one concludes that $\partial F/\partial\Delta > 0$. In this case sign $H = $ sign $\partial G/\partial I$, where sign stands for the sign function. It then follows that $H > 0$ implies $D_{kk}^p > 0$ (densification) and $H < 0$ implies $D_{kk}^p < 0$ (dilation). On $H = 0$, $D_{kk}^p = \partial G/\partial I = 0$. In the $I, \sqrt{J}$-plane the curve $\partial G/\partial I = 0$ defines the critical states; see Section 4. Note that when $h \neq 0$ then sign H is not necessarily equal to sign $\partial G/\partial I = $ sign D_{kk}^p.

Returning to the general case, we note that with the aid of (3.3) the basic rate equation for the *distortional* part of the deformation rate becomes

$$D_{ij}' = \frac{\overset{*'}{\sigma}_{ij}}{2\mu} + \frac{1}{h+h_1} \frac{\sigma_{ij}'\sigma_{kl}'}{4J} \overset{*}{\sigma}_{kl} - \frac{\partial F/\partial I}{2(h+h_1)\sqrt{J}} \overset{*}{\sigma}_{kk}\sigma_{ij}'. \tag{3.5}$$

This equation has some of the attributes of a constitutive relation which has been proposed by Rudnicki and Rice[2] and which has been obtained by the generalization of a deformation type plasticity theory. The corresponding equation of [2] can be expressed as

$$D_{ij}' = \left(\frac{1}{\mu} + \frac{1}{2\bar{h}_1}\right) \overset{*'}{\sigma}_{ij} + \left(\frac{1}{h} - \frac{1}{\bar{h}_1}\right) \frac{\sigma_{ij}'\sigma_{kl}'}{4J} \overset{*}{\sigma}_{kl} + \frac{\bar{\mu}}{6h\sqrt{J}} \overset{*}{\sigma}_{kk}\sigma_{ij}', \tag{3.6}$$

where the shear modulus is denoted by μ, the internal friction coefficient by $\bar{\mu}$, and $\bar{h}_1$ here is the second modulus. A basic difference between the two equations is that in (3.6) the introduction of the second modulus also affects the elastic response, whereas in (3.5) the elastic and plastic parts are completely kept apart. In (3.6) the *effective* elastic shear modulus is

---

[†]From eqn (2.11) it can be concluded that if H tends to zero, then for D_{ij}^p to remain bounded, the quantity inside the parentheses must vanish. Since this quantity is given by $\overset{*}{\sigma}_{ij}\partial f/\partial\sigma_{ij}$ we see that, in this case, the stress rate becomes tangent to the yield surface (perfect plasticity).

predicted to increase with plastic deformation, and hence the relative values of the strain rate components depend on the relative values of the stress rates. In addition, eqn (3.5) presents a proper flow theory plasticity whereas (3.6) is deduced by generalizing linear elasticity equations. The hardening parameter, H, and its constituents, h and h_1 in (3.5), have clear physical interpretations, and may be correlated directly with physically observed responses of compressible frictional inelastic materials, see next section for an illustration. A similar comment applies to the other parameters which enter the present theory.

Before we compare our results with those of Wilde[3], we briefly discuss an alternative formulation of the theory in terms of the effective plastic strain, eqn (3.1)$_2$. To this end, instead of the plastic distortional work, we introduce the total "effective" plastic strain, Hill[5], as

$$\bar{\gamma} = \int_0^\theta (2D_{ij}^{p'} D_{ij}^{p'})^{1/2} \, d\theta', \tag{3.7}$$

and set

$$g = \sqrt{J} + \bar{G}(I, \Delta, \bar{\gamma}), \quad f = \sqrt{J} - \bar{F}(I, \Delta, \bar{\gamma}), \tag{3.8}$$

for the flow potential and the yield function, respectively. Now, following the same procedure as before, we obtain equations similar to (2.10) and (2.11), except that the functions G and F must be replaced by $\bar{G}$ and $\bar{F}$, respectively. For the hardening parameter, H, however, we obtain

$$H = 3 \frac{\rho_0}{\rho} \frac{\partial \bar{G}}{\partial I} \frac{\partial \bar{F}}{\partial \Delta} + \frac{\partial \bar{F}}{\partial \bar{\gamma}}, \tag{3.9}$$

and notice that $\partial \bar{F}/\partial \bar{\gamma} = \partial \bar{\tau}/\partial \bar{\gamma} = h$ is indeed the slope of the shear stress-plastic shear strain curve in a simple shear test.

Wilde[3] considers a small strain plasticity theory with normality and associative flow rule. The last assumption implies that the functions g and f are identical. In view of the assumption of small deformations, the total linearized elastic and plastic strains are additive, i.e. $\epsilon_{ij} = \epsilon_{ij}^e + \epsilon_{ij}^p$, where ϵ stands for the linearized strain. Then, instead of the total effective plastic strain, $\bar{\gamma}$, and the total plastic volumetric strain, Δ, one may use, respectively, $N = ((1/2)\epsilon_{ij}^{p'} \epsilon_{ij}^{p'})^{1/2}$ and ϵ_{ii}^p, in the yield function, arriving at Wilde's equations. As pointed out before, most problems associated with the inelastic behavior of granular materials involve finite deformations. Moreover, there is no reason to believe that the dilatancy factor, $3\partial G/\partial I$, and the effective frictional factor, $-3\partial F/\partial I$, should always be equal. In fact, the latter quantity is always positive for frictional materials, whereas the former may be positive, negative or zero, depending on whether D_{kk}^p is positive, negative or zero. Therefore, the theory presented here ought to provide a suitable general setting for the description of mechanical properties of soil and rock masses in particular, and other dilatant plastic materials in general.

4. APPLICATION: TRIAXIAL TEST OF SOILS

We consider in some detail a possible application of the theory to the triaxial test commonly used to study the mechanical response of soils. We assume an initial homogeneous stress state defined by

$$\sigma_{11} = \sigma_1, \quad \sigma_{22} = \sigma_{33} = \sigma_2, \quad \text{all other } \sigma_{ij} = 0, \quad \sigma_1 > \sigma_2, \tag{4.1}$$

and, in line with practice in soil mechanics, regard compression and contraction positive and tension and extension negative. The deviatoric components of the stress are

$$\sigma_{11}' = \frac{2}{3}(\sigma_1 - \sigma_2), \quad \sigma_{22}' = \sigma_{33}' = -\frac{1}{3}(\sigma_1 - \sigma_2), \tag{4.2}$$

and hence,

$$I = \sigma_1 + 2\sigma_2, \quad J = \frac{1}{3}(\sigma_1 - \sigma_2)^2. \tag{4.3}$$

Since, for granular materials consisting of rigid or almost rigid particles, the strains are totally or essentially inelastic, we only consider the plastic strain rates, D_{ij}^p, and for simplicity drop out the superimposed p in the sequel. Then, from (2.10), (2.11), and in view of (4.1), it follows that $D_{11} = D_1$, and $D_{22} = D_{33} \equiv D_2$, are the only nonzero strain rate components, so that the deviatoric components of the strain rates are,

$$D'_{11} = \frac{2}{3}(D_1 - D_2), \quad D'_{22} = D'_{33} = -\frac{1}{3}(D_1 - D_2). \tag{4.4}$$

Denote by Λ_i the stretch† in the x_i-direction, $i = 1, 2, 3$. Then, by definition and in view of the sign convention, we have $-D_i = (\ln \Lambda_i)^{\cdot}$ and

$$D_1 - D_2 = [\ln(\Lambda_2/\Lambda_1)]^{\cdot} > 0. \tag{4.5}$$

We shall use

$$\epsilon = \frac{2}{3}\ln(\Lambda_2/\Lambda_1) \tag{4.6}$$

as the "time parameter", and note that when $\Lambda_1 = \Lambda_2 = 1$ (no deformation), we have $\epsilon = 0$. Observe that since $\sigma_1 > \sigma_2$, we have $\Lambda_1 < 1$ and $\Lambda_2 > 1$, i.e. contraction in the x_1-direction, and expansion in the x_2- and x_3-directions. Hence, for this kind of loading, $\Lambda_2/\Lambda_1 > 1$, which implies that $\epsilon > 0$, and, in view of (4.5), ϵ is monotone increasing for continued deformation. In what follows only deformations of this kind will be considered; however the results can easily be modified if the sample extends in the x_1-direction and contracts in the x_2- and x_3-directions, in which case the roles of Λ_1 and Λ_2 on one hand, and D_1 and D_2 on the other hand, must be reversed. Note that in terms of Λ_1 and Λ_2 the volumetric strain is

$$\Delta = 1 - \Lambda_1 \Lambda_2^2. \tag{4.7}$$

In soil mechanics the state of stress in a triaxial test is usually characterized by pressure, p, and distortional stress, q,

$$p = \frac{1}{3}(\sigma_1 + 2\sigma_2) = \frac{1}{3}I, \quad q = (\sigma_1 - \sigma_2) = \sqrt{(3J)}. \tag{4.8}$$

The state of deformation is characterized by the rate of volumetric strain, $\dot{v}/v$, measured per unit current volume, and the distortional strain, $\dot{\epsilon}$,

$$\dot{v}/v = D_1 + 2D_2, \quad \dot{\epsilon} = \frac{2}{3}(D_1 - D_2) \equiv D'_{11}. \tag{4.9}$$

In the sequel we shall use (p, q) to represent the state of stress and $(\dot{v}/v, \dot{\epsilon})$ to represent the strain rate.

The rate of distortional work per unit *current* volume is

$$\frac{\rho}{\rho_0}\dot{\xi} = \frac{2}{3}(\sigma_1 - \sigma_2)(D_1 - D_2) = q\dot{\epsilon}. \tag{4.10}$$

---

†Λ_i is the length of an element in the current configuration, ds_i, divided by the corresponding initial length, dS_i.

On the other hand, by definition, [eqns (2.6), (2.8) and (2.9)], we have

$$\frac{p}{p_0}\dot{\xi} = \frac{1}{\sqrt{3}}\frac{q}{H}\left(\frac{1}{\sqrt{3}}\dot{q} - \frac{\partial F}{\partial p}\dot{p}\right) = \frac{1}{\sqrt{3}}q\dot{\lambda} > 0. \tag{4.11}$$

From (4.10) and (4.11) it now follows that

$$\frac{dq}{d\epsilon} - \sqrt{3}\frac{\partial F}{\partial p}\frac{dp}{d\epsilon} = 3H. \tag{4.12}$$

This equation relates q and p. If the work-hardening parameter H is established experimentally or by other means, then (4.12) can be used directly; we shall illustrate this in the sequel; see eqn (4.30) and the corresponding discussions.

The dilatancy factor, $3\partial G/\partial I = \partial G/\partial p$, can be given a clear physical interpretation in the present special case. From (2.6)$_4$, (2.12) and (4.10), it follows that

$$\sqrt{3}\frac{\partial G}{\partial p} = \frac{3}{2}\frac{D_1 + 2D_2}{D_1 - D_2} = \frac{1}{v}\frac{\dot{v}}{\dot{\epsilon}} = \frac{1}{v}\frac{dv}{d\epsilon} \tag{4.13}$$

which indicates that $\sqrt{3}\partial G/\partial p$ is the rate of volumetric strain, $\dot{v}/v$, per unit rate of distorional strain, $\dot{\epsilon}$. Hence, the dilatancy factor can be established experimentally as suggested by (4.13); note that in the present case the denominator in the right-hand side of (4.13) is positive.

Let e denote the void ratio, i.e. the ratio of the void volume, V_v, to the volume of the solid, V_s, contained within a sample of total volume $V_v + V_s$, $e = V_v/V_s$. Then, by definition the volumetric strain, Δ, is related to the void ratio by

$$\Delta = \frac{e_0 - e}{1 + e_0}, \tag{4.14}$$

where e_0 is the initial value of the void ratio; note that, in view of the sign convention, Δ is defined by $(v_0 - v)/v_0$ where v is the current volume and v_0 is the initial volume of the sample.

From (2.6)$_{3,4}$ and (2.12) we obtain

$$\dot{\Delta} = \frac{p_0}{p}D_{ii} = \frac{\dot{\xi}}{\sqrt{J}}\frac{\partial G}{\partial p} \tag{4.15}$$

which can be integrated to yield

$$\Delta = \int_0^\xi \frac{1}{\sqrt{J}}\frac{\partial G}{\partial p}d\xi', \tag{4.16}$$

with the initial condition $\Delta = 0$ at $\xi = 0$. Equation (4.16) is valid in general. It can be further reduced for the triaxial state of strain considered here. To this end we note that either (4.15) or (4.13) can be written as

$$\frac{d\Delta}{1 - \Delta} = \sqrt{3}\frac{\partial G}{\partial p}d\epsilon \tag{4.17}$$

which, upon integration, gives

$$\Delta = 1 - \exp\left\{-\sqrt{3}\int_0^\epsilon \frac{\partial G}{\partial p}d\epsilon'\right\}. \tag{4.18}$$

With the aid of (4.14) it now follows that

$$e = e_0 - (1 + e_0)\left[1 - \exp\left\{-\sqrt{3}\int_0^\epsilon \frac{\partial G}{\partial p}d\epsilon'\right\}\right]. \tag{4.19}$$

It is commonly accepted that a monotone and continuous shearing of cohesionless sand leads to a void ratio, e_c, called critical, which only depends on the confining pressure and the grain size distribution and shape, but is indepednent of the initial value of the void ratio. This means that in a continuous monotone deformation, the dilatancy factor $\partial G/\partial p$ must approach zero. We hence set

$$K = \lim_{\epsilon \to \infty} \exp\left\{ -\sqrt{3} \int_0^\epsilon \frac{\partial G}{\partial p} \, d\epsilon' \right\},$$ (4.20)

and then obtain

$$e_c = e_0 - (1 + e_0)(1 - K),$$

from which it follows that

$$K = \frac{1 + e_c}{1 + e_0}.$$ (4.21)

Hence we obtain

$$\sqrt{3} \int_0^\infty \frac{\partial G}{\partial p} \, d\epsilon' = \ln\left(\frac{1 + e_0}{1 + e_c} \right)$$ (4.22)

which shows that there is a net amount of densification or dilatancy depending on whether $e_0 > e_c$ (loose sand) or $e_0 < e_c$ (dense sand). Figure 1 shows the observed variation of e with the strain, ϵ. Curve (1) is for loose sand, $e_0 > e_c$, for which e decreases monotonically with increasing ϵ, approaching e_c asymptotically. In this case $\partial G/\partial p$ remains positive (continuous densification). Curve (2) of Fig. 1, on the other hand, is for dense sand, $e_0 < e_c$. In this case experiment shows that, similar to the case of loose sand, there is an initial densification which is, however, followed by dilatancy. Hence, $\partial G/\partial p$ is initially positive, but for dense sand, it becomes zero at a certain ϵ, and then is negative as ϵ is increased, approaching zero asymptotically. For this case, there is always a net amount of dilatancy. We shall show in the sequel that all these experimentally observed facts are contained in the constitutive model which has been developed in this paper.

4.1 A model for cohesionless sands

We shall now attempt to construct a relation between the dilatancy factor, $\partial G/\partial p$, and the coefficient of internal friction, $\partial F/\partial p$, for cohesionless sands. To this end we observe that the *total* rate of plastic work, $\dot{w}_p$, measured per unit *current* volume is

$$\dot{w}_p = p\dot{v}/v + q\dot{\epsilon}.$$ (4.23)

If the only source of dissipation is internal friction due to sliding, the above rate of work must equal the rate of frictional loss.
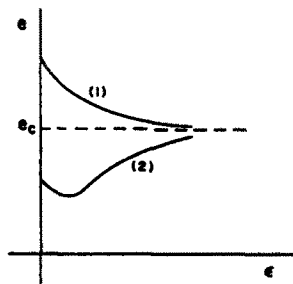

Fig. 1. Variation of the void ratio with strain in a triaxial test; Curve (1) is for loose, and Curve (2) for dense sands.
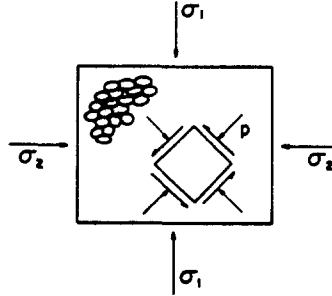
Fig. 2. Biaxial state of stress.

The calculation of the rate of frictional loss requires careful consideration of the relative motion of the grains, and is indeed a complicated problem. We therefore consider a simple (approximate) approach instead, as follows.

As a motivation, first consider *biaxial* defromation of cylindrical rods, plane strain problem, where $D_{33} = 0$, see Fig. 2. In this case the rate of change of area is $\dot{a} = D_1 + D_2$, and the two-dimensional deviatoric strain rates are $D'_{11} = (1/2)(D_1 - D_2)$ and $D'_{22} = -(1/2)(D_1 - D_2)$. The hydrostatic pressure becomes $p = (1/2)(\sigma_1 + \sigma_2)$. Consider now a biaxial deformation where the axial strain rates are equal to the deviatoric ones, D'_{11} and D'_{22}. The sample undergoes plane strain pure shearing and, since on planes making a $45°$ angle with the principal stress axes the normal stress is equal to the hydrostatic pressure, the frictional stress on these planes would be $\tau_f = (\partial F/\partial p)p$, $\partial F/\partial p$ being the coefficient of friction. Hence, the rate of frictional work per unit current volume becomes $\tau_f(|D'_{11}| + |D'_{22}|) = 2\tau_f D'_{11} = \tau_f(D_1 - D_2)$.

In the triaxial case with $D_{11} = D_1$, $D_{22} = D_{33} = D_2$, we add the contribution for motions in the x_1, x_2-, x_2, x_3- and x_1, x_3-planes, arriving at

$$\dot{w}_f \approx \frac{\partial F}{\partial p} p(|D_{11} - D_{22}| + |D_{22} - D_{33}| + |D_{33} - D_{11}|)$$

$$= 2\frac{\partial F}{\partial p} p(D_1 - D_2) = 3\frac{\partial F}{\partial p} p\dot{\epsilon}. \qquad (4.24)$$

If we now equate the rate of plastic work with the rate of frictional loss, and consider (4.13), we obtain

$$\sqrt{3}\frac{\partial G}{\partial p} = 3\frac{\partial F}{\partial p} - \frac{q}{p}. \qquad (4.25)$$

This relates the dilatancy factor with the coefficient of internal friction. Equation (4.25) may be regarded as a generalization of eqn (5.21a) of Schoefield and Wroth[4]. It however shows that the concepts of internal friction and dilatancy are not compatible with the assumption of associative flow rule which has been used by these authors, and also be Wilde[3].

Since the friction coefficient, $\partial F/\partial p$, is positive, eqn (4.25) shows that under a constant confining pressure, $p = \text{constant}$, the dilatancy factor, $\partial G/\partial p$, is always initially, i.e. at $q = 0$, positive. Hence initially the sample tends to densify, as shown for both curves (i.e. loose sand and dense sand) in Fig. 1. It is remarkable that the theory yields this experimental fact as one of its immediate consequence.

In the p, q-plane the curve

$$3\frac{\partial F}{\partial p} p - q = 0 \qquad (4.26)$$

is the locus of points on which $\partial G/\partial p = \dot{v} = 0$, i.e. it is the critical curve which passes through the origin, see Fig. 3. If the coefficient of friction, $\partial F/\partial p$, is assumed to be constant, we obtain the critical line introduced by Schofield and Wroth[4].
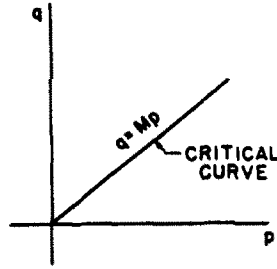
Fig. 3. The critical curve in the q, p-plane for cohesionless sand.

Consider now the hardening parameter (2.9), and in view of (4.6), (4.7) and (4.8) obtain

$$H = \frac{1}{\sqrt{3}}\left[\left(3\frac{\partial F}{\partial p} - \frac{q}{p}\right)(1-\Delta)\frac{\partial F}{\partial \Delta} + \frac{\partial F}{\partial \epsilon}\right], \qquad (4.27)$$

where (4.25) is used. The last term in the right-hand side represents hardening due to the distortional plastic work, i.e. $h = (\partial F/\partial \epsilon)/\sqrt{3}$, see (3.2). The remaining terms on the right-hand side of (4.27), on the other hand, represent hardening due to changes in density. The quantity $(1-\Delta)\partial F/\partial \Delta$ is always positive, as it represents hardening due to volumetric contraction; note that F increases with increasing Δ, i.e. with plastic compaction.

For simplicity we set

$$3\frac{\partial F}{\partial p} = M > 0, \quad a = \sqrt{3}(1-\Delta)\frac{\partial F}{\partial \Delta} > 0, \quad \hat{h} = \sqrt{3}\frac{\partial F}{\partial \epsilon}, \qquad (4.28)$$

and reduce (4.27) to

$$H = \frac{1}{3}\left[a\left(M - \frac{q}{p}\right) + \hat{h}\right]; \qquad (4.29)$$

note that a, M and $\hat{h}$ are, in general, functions of ϵ. We now substitute from (4.29) into (4.12) to arrive at

$$\frac{dp}{d\epsilon} - \frac{\sqrt{3}}{3}M\frac{\partial p}{\partial \epsilon} = a\left(M - \frac{q}{p}\right) + \hat{h}. \qquad (4.30)$$

This is our main differential equation. It includes all commonly observed behavior of cohesionless sands in triaxial tests with monotonically changing loading conditions. To show this, we shall consider a triaxial test under constant confining pressure, p = constant. We note, however, that qualitatively the results will be the same for a triaxial test in which σ_2 is held fixed.

At constant pressure the differential equation (4.30) becomes

$$\frac{dq}{d\epsilon} = (aM + \hat{h}) - \frac{a}{p}q. \qquad (4.31)$$

We shall now examine qualitatively the solution of this differential equation with the initial condition

$$q = 0 \text{ at } \epsilon = 0 \qquad (4.32)$$

for two possible behavior of the work-hardening function $\hat{h} = \hat{h}(\epsilon)$. These are sketched in Fig. 4(a) by Curves (1) and (2). We assume, moreover, that the positive quantity aM remains essentially constant.
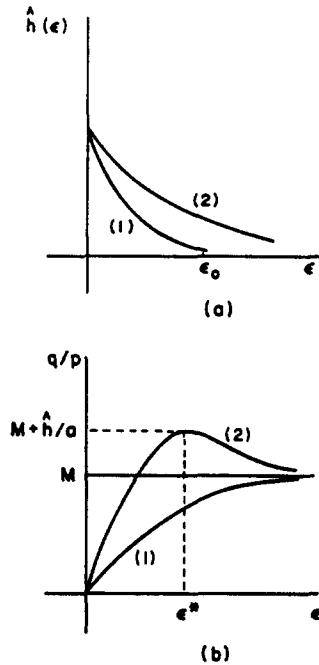
Fig. 4. (a) Variation of the distorsional hardening parameter with strain; (b) Variation of the normalized differential stress with strain; Curves (1) are for loose and Curves (2) for dense samples.

In the case of Curve (1), $\hat{h}$ drops to zero very quickly and is assumed to be essentially zero for $\epsilon > \epsilon_0$ with† $\epsilon_0 \ll p/a$. Then from (4.31) it is clear that in the q, ϵ-plane one obtains a solution similar to Curve (1) of Fig. 4(b), where q increases monotonically from zero approaching $(q/p) = M$ asymptotically. This is the response of loose sand, $e_0 > e_c$. From this and eqn (4.19) written as

$$e = e_0 - (1 + e_0)\left[1 - \exp\left\{-\int_0^\epsilon (M - q/p)\, d\epsilon'\right\}\right], \tag{4.33}$$

it then follows that the void ratio e decreases monotonically, approaching a constant value, e_c, as shown by Curve (1) in Fig. 1.

The assumption that the material hardening due to distortional work, i.e. $\hat{h} = \sqrt{3}(\partial F/\partial\epsilon)$, should behave for loose sand in a manner sketched by Curve (1) of Fig. 4(a), may be justified if we consider the fact that in this case there is a substantial amount of densification and, therefore, hardening due to the density changes is very dominant; in fact, for a very loose sand, one may totally ignore the effect of $\hat{h}$, and consider a model with only density-hardening.

In Fig. 4(a) Curve (2) shows a variation for $\hat{h}$ which, although monotonically decreasing with increasing ϵ, does not approach zero fast enough. Therefore, the function $\hat{h}$ will affect the qualitative behavior of the solution of eqn (4.31). For a and M positive constants, this is sketched by Curve (2) in Fig. 4(b). Since $\hat{h}$ approaches zero for sufficiently large ϵ, the solution curve of (4.31), in the q, ϵ-plane again approaches asymptotically the line $q/p = M$, as shown by Curve (2) in Fig. 4(b). However, in this case q/p increases monotonically, becoming equal to M for a certain value of ϵ at which $\hat{h}(\epsilon)$ is still finite. Hence, q/p continues to increase until the right-hand side of eqn (4.31) is zero at $\epsilon = \epsilon^*$, after which, because of the monotone decreasing nature of $\hat{h}$, q/p decreases monotonically, approaching asymptotically from above, $q/p = M$. As is well known, this is precisely the observed behavior of dense sand. Moreover, with this variation of q/p with respect to ϵ, eqn (4.33) immediately reveals that the void ratio in this case varies with ϵ in a manner shown by Curve (2) of Fig. 1. Here, as q/p increases from zero, the void ratio decreases, attaining its minimum value when $q/p = M$. After this the void ratio begins to increase, attaining the initial value e_0 at point where $\int_0^\epsilon (M - q/p)\, d\epsilon' = 0$. After this point e

†Note the role of hydrostatic pressure.

increases monotonically, attaining the critical value e_c asymptotically, see Curve (2) of Fig. 1. For dense sand, therefore, both the density-hardening and the hardening due to plastic distortion play dominant roles. The present model seems to adequately represent the observed behavior of cohesionless sands.

4.2 Model with cohesion

In the preceding case we have assumed cohesionless granular materials, and hence resistance to sliding stems only from frictional effects. The model may be generalized somewhat by including the cohesive effects. In a simplified attempt one may modify the frictional resistance by the addition of a cohesive force, $(1/3)C$, which may be regarded to depend on p, Δ and ϵ, or one may assume it to be a constant, as the situation may dictate. The rate of frictional work is now modified to

$$\dot{w}_f = 3\left(\frac{\partial F}{\partial p}p + \frac{1}{3}C\right)\dot{\epsilon}.$$

(4.34)

Equations (4.25) and (4.26) now, respectively, become

$$\sqrt{3}\frac{\partial G}{\partial p} = 3\frac{\partial F}{\partial p} - \frac{q-C}{p},$$

(4.35)

$$3\frac{\partial F}{\partial p}p - (q-C) = 0.$$

(4.36)

The critical curve defined by (4.36) no longer passes through the origin in the p, q-plane, but intersects the q-axis at $q = C$ (see Fig. 5). This is compatible with experimental observation on cohesive soils.

In the present case the hardening parameter, H, becomes

$$H = \frac{1}{\sqrt{3}}\left\{\left(3\frac{\partial F}{\partial p} - \frac{q-C}{p}\right)\left[(1-\Delta)\frac{\partial F}{\partial\Delta}\right] + \frac{\partial F}{\partial\epsilon}\right\}.$$

(4.37)

The presence of cohesion therefore, has the effect of modifying the frictional coefficient $M = 3\partial F/\partial p$. Depending on how the cohesion factor C, which is a non-negative quantity, varies as ϵ is increased, we obtain a modified response in the q, ϵ-plane, but qualitatively the results are similar to those already discussed for cohesionless sand, and therefore will not be explored any further here.

4.3 Simple shear

It is seen that the constitutive relation developed in this paper seems to account for the observed mechanical responses of granular materials in triaxial tests. It is easy to verify that a similar conclusion is obtained for the simple shear test of this kind of materials. In fact, in this case a more rigorous estimate for the rate of frictional loss can be obtained. Hence, if the shear stress is denoted by τ and the shear strain by γ, then, for the simple shear test, one has: $J = \tau^2$,
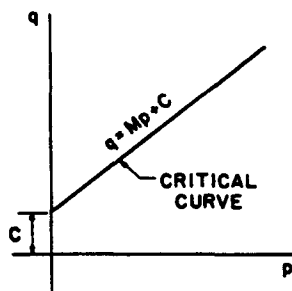

Fig. 5. The critical curve in the q, p-plane for cohesive soils.

$D_{12} = D_{21} = (1/2)\dot\gamma$, $\dot{w}_p = p\dot{v}/v + \tau\dot\gamma$, and $\dot{w}_f = (\partial F/\partial p)p\dot\gamma$. Hence, instead of eqn (4.25), we now have

$$\frac{\partial G}{\partial p} = \frac{\partial F}{\partial p} - \frac{\tau}{p}. \tag{4.38}$$

In view of (2.6)$_4$, we also obtain

$$\frac{p}{\rho_0}\dot\xi = \tau\dot\gamma = \tau\dot\lambda = \frac{\tau}{H}\left(\dot\tau - \frac{\partial F}{\partial p}\dot p\right)$$

which yields

$$\frac{d\tau}{d\gamma} - \frac{\partial F}{\partial p}\frac{dp}{d\gamma} = H, \tag{4.39}$$

where H, the work-hardening parameter, becomes

$$H = \left(\frac{\partial F}{\partial p} - \frac{\tau}{p}\right)(1-\Delta)\frac{\partial F}{\partial \Delta} + \frac{\partial F}{\partial \gamma}$$

$$= \frac{a}{\sqrt 3}\left(\frac{1}{3}M - \frac{\tau}{p}\right) + h, \tag{4.40}$$

where a and M are as defined by (4.28), and h is the tangent modulus in simple shear, as defined in Section 3.

Hence, except for slight modifications of coefficients, in simple shear equations similar to those of triaxial test are obtained. Therefore the form of the solution will be the same as that of the triaxial test.

4.4 Comparison with experiments

Here we shall examine in the light of our theory, some experimental results on triaxial tests of crushed Westerly granite and Ottawa sand, reported by Zoback and Byerlee[9, 10].

Figure 6 reproduces Fig. 1 of Zoback and Byerlee[9, p. 292], and shows the differential stress, q in the present notation, and the change in void volume per unit initial void volume, as functions of the axial strain $\Delta l/l$. As suggested by our theory, we have replotted these experimental results in Figs. 7 and 8: Figure 7 represents the *normalized* differential stress, q/p, vs the strain ϵ defined by eqn (4.6); while Fig. 8 represents the void ratios as functions of the same strain measure.† As is seen from Fig. 7, all experimental results for crushed Westerly granite in this new representation, essentially fall on the same stress-strain curve. Moreover, from Fig. 8 the variation of void ratios seems to follow a single pattern, their difference essentially being due to the initial value of the corresponding void ratio.

To fit these experimental data with a minimum number of parameters, we shall use the simplest possible form for the material functions, and assume in eqn (4.31) that a/p and M are both constants and that the hardening function $\hat h$ has the following simple exponential form:

$$\hat h = h_0 e^{-\beta\epsilon}, \tag{4.41}$$

β being a constant. Hence eqn (4.31) can be integrated to yield

$$\frac{q}{p} = M\left[1 - \exp\left\{-\frac{a}{p}\epsilon\right\}\right] + \frac{h_0/p}{a/p - \beta}\left[\exp\{-\beta\epsilon\} - \exp\left\{-\frac{a}{p}\epsilon\right\}\right]. \tag{4.42}$$

We shall now establish the values of the parameters M, a/p, h_0/p, and β, for the experimental results reported in Figs. 7 and 8.

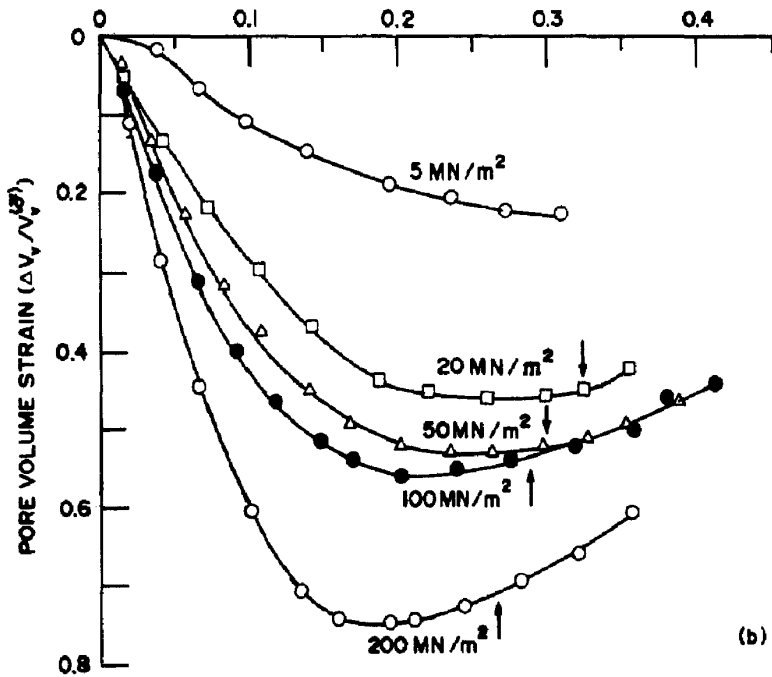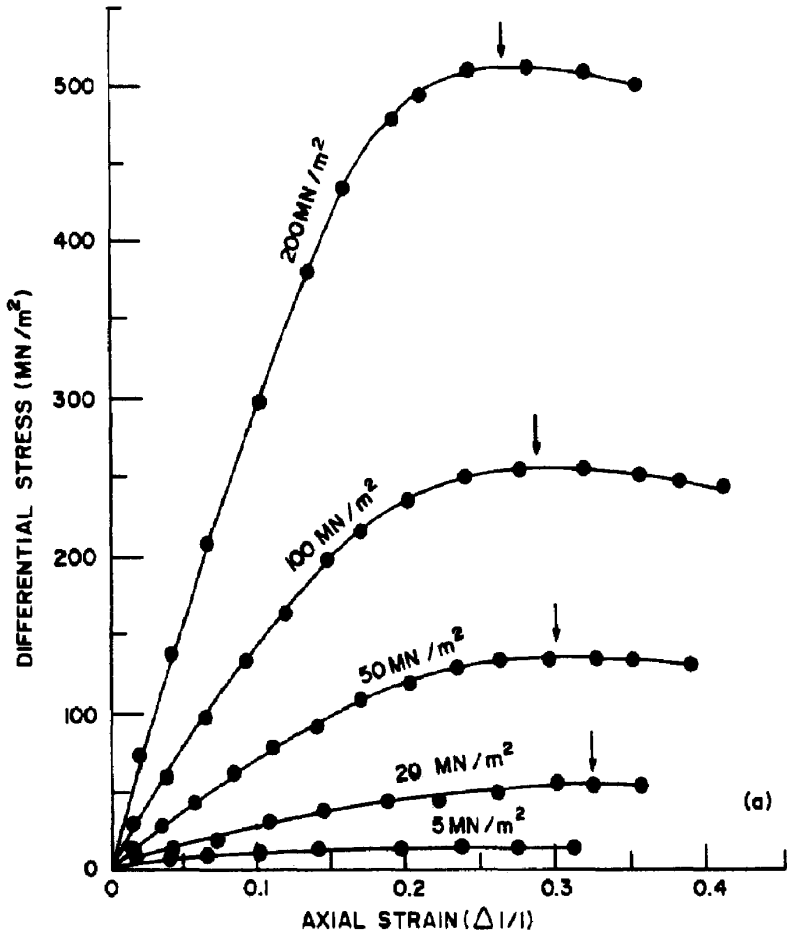†We have replotted only those points for which all the needed data were available.

Fig. 6. Deformational behavior of crushed Westerly granite in triaxial compression. (a) Differential stress vs axial strain; (b) Void volume strain (measured per unit initial void volume) vs axial strain; (Courtesy of Zoback and Byerlee[9], p. 292, Fig. 1).
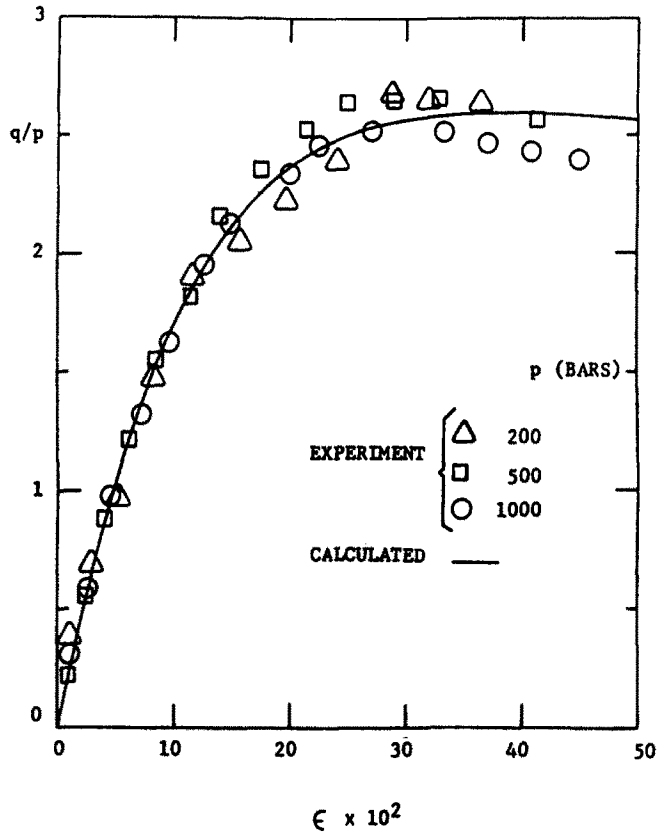
Fig. 7. Normalized differential stress, q/p vs the strain, $\epsilon = (2/3)\ln(\Lambda_2/\Lambda_1)$, in triaxial tests of crushed Westerly granite; Experimental data from Zoback and Byerlee [9]; The theoretical (solid) curve displays eqn (4.42) with $M = 2.4$, $B = (a/p)M + (h_0/p) = 26$, $a/p = 7$ and $\beta = 5$.
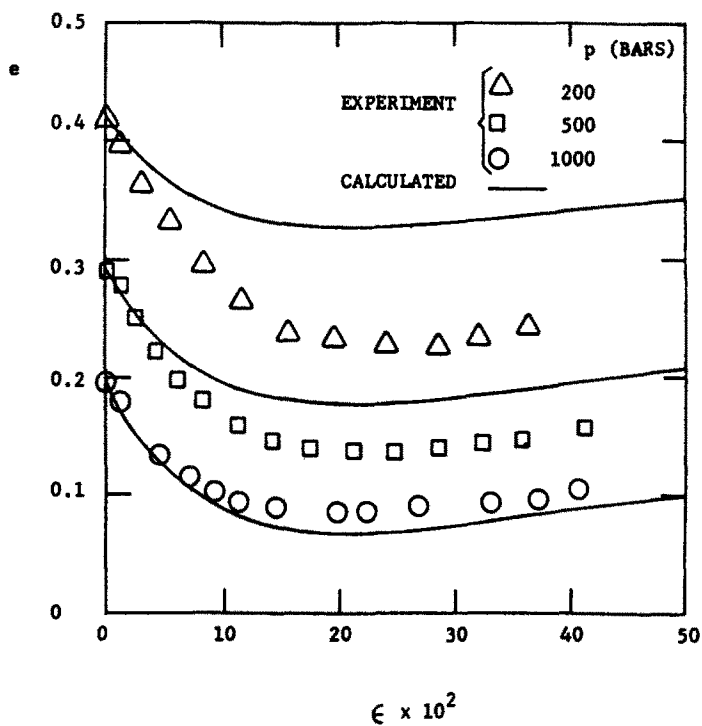
Fig. 8. Void ratio, e, vs the strain ϵ in triaxial tests of crushed Westerly granite; Experimental data from Zoback and Byerlee [9]; The theoretical (solid) curves display eqn (4.33) for the q/p, ϵ-relation of Fig. 7.

Since $M = 3\partial F/\partial p$, and since $\partial F/\partial p$ is the coefficient of overall friction in shear, we can identify the possible range of variation of M from the frictional strength of rocks, reported by Byerlee[11, 12], which has been reproduced as Fig. 3 in[9]. From this result it is evident that for the low-pressure range, $\partial F/\partial p$ varies somewhere between 0.6 and 1. On the other hand, the curve q/p, according to the theory, crosses the line $q/p = M$ at the point where the void ratio has its minimum value, see the discussion at the end of Section 4.1. From the experimental results the crossing occurs for M between 2.3 and 2.7. If we take $\partial F/\partial p = 0.8$, as suggested by experimental results, then we have $M = 2.4$.

We evaluate eqn (4.31) at $\epsilon = 0$, to obtain the initial slope of the stress-strain curve as

$$B = \left[\frac{1}{p}\frac{dq}{d\epsilon}\right]_{\epsilon=0} = \frac{a}{p}M + \frac{h_0}{p}. \tag{4.43}$$

Comparison with the data reported in Fig. 7 shows that $B \approx 26$. Moreover, $a/p = 7$ and $\beta = 5$ seem to be adequate estimates in the present context.

With the above values of the coefficients, the curve in Fig. 7 displays eqn (4.42), which seems to fit the experiments. It is experimentally very difficult to obtain reliable data after the peak stress is attained, because the sample then is unstable. Therefore we have not tried to force the theoretical curve to follow closely the experimental trend after the peak stress. However, it should be noted that the theoretical curve in Fig. 7 displays a peak stress and then drops asymptotically to $q/p = M = 2.4$.

From eqn (4.33) and (4.42) we can now calculate the corresponding void ratios. The theoretical results are shown by solid curves in Fig. 8. Comparison for $p = 500$ and 1,000 bars is good, but for the lower pressure, i.e. $p = 200$ bars, only the trend is displayed.

The experimental results reported by Zoback and Byerlee[10] for Ottawa sand may be divided into two categories: those associated with $p = 1,000$ and 1,500 bars, and the others associated with lower pressures. Although it is difficult to precisely ascertain from the reported results, the higher pressure data seem to suggest the existence of a peak stress, whereas the lower pressure data do not. Figures 9 and 10 are the plots of q/p vs ϵ.

For Fig. 9 we have set $M = 2.4$, $B = 32$, $a/p = 9$ and $\beta = 7$, and from eqn (4.42) plotted the theoretical results by a solid curve. This is an excellent fit to the experimental results, because not only are the experimental data for the stress-strain relation closely followed, but also the theory predicts very nicely the variation in the corresponding void ratio for $p = 1,000$ bars, as shown in Fig. 11, unfortunately we did not have all the necessary experimental data corresponding to $p = 1,500$ bars.

The experimental results for lower pressures in Fig. 10 are fitted by a curve associated with the theoretical results for *loose* sand with $\hat{h} = 0$. In this case we have from (4.42),

$$\frac{q}{p} = M\left[1 - \exp\left\{-\frac{a}{p}\epsilon\right\}\right] \tag{4.44}$$

which involves only two material parameters, and does not display a peak stress. To obtain the solid curve shown in Fig. 10, we have set $M = 2.3$ and $a/p = 15$. In Fig. 11 the corresponding variation of the void ratio is shown by the solid curve; the upper curve. It closely follows the data for 350 and 500 bar pressure, but not those for 200 bar pressure.

In view of the fact that the experiments used here were not conducted to test the present theory, the comparison seems to be good. We are, however, in the process of obtaining additional experimental facts, in order to verify the theoretical predictions.

4.5 Additional comments

In recent years there has been a considerable effort devoted to the understanding of the precursory events which may lead to unstable fault movements and consequent earthquakes. A summary of this and related mechanical matters is given by Rice[13] and by Stuart[14], where references to other works can be found. In[15] Stuart considers a constitutive model for the fault gauge, which is essentially in the form of Curve (2) of Fig. 4(b), i.e. a dense granular material under large confining pressure. He then gives a qualitative account of the correspond-
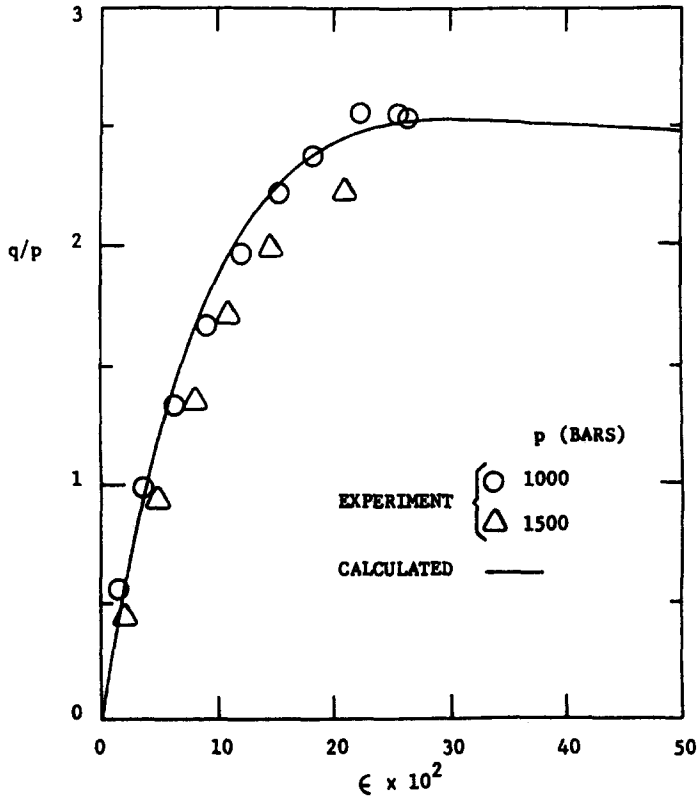
Fig. 9. Normalized differential stress, q/p, vs the strain, $\epsilon = (2/3) \ln(\Lambda_2/\Lambda_1)$, in triaxial tests of Ottawa sand; Experimental data from Zoback and Byerlee[10]; The theoretical (solid) curve displays eqn (4.42) with $M = 2.4$, $B = (a/p)M + (h_0/p) = 32$, $a/p = 9$ and $\beta = 7$.
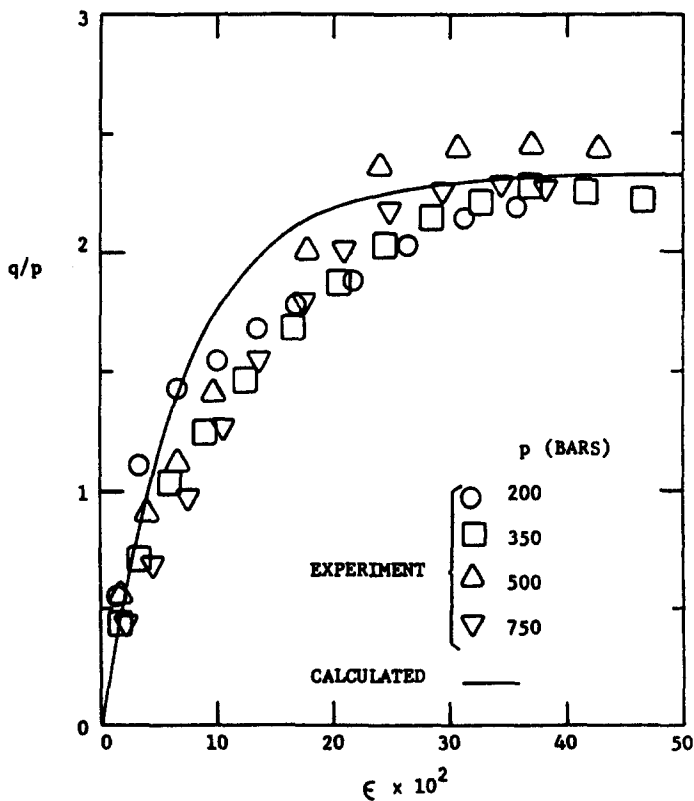

Fig. 10. Normalized differential stress, q/p, vs the strain, $\epsilon = 2/3 \ln(\Lambda_2/\Lambda_1)$, in triaxial tests of Ottawa sand; Experimental data from Zoback and Byerlee[10]; The theoretical (solid) curve displays eqn (4.44) with $M = 2.3$ and $a/p = 15$.
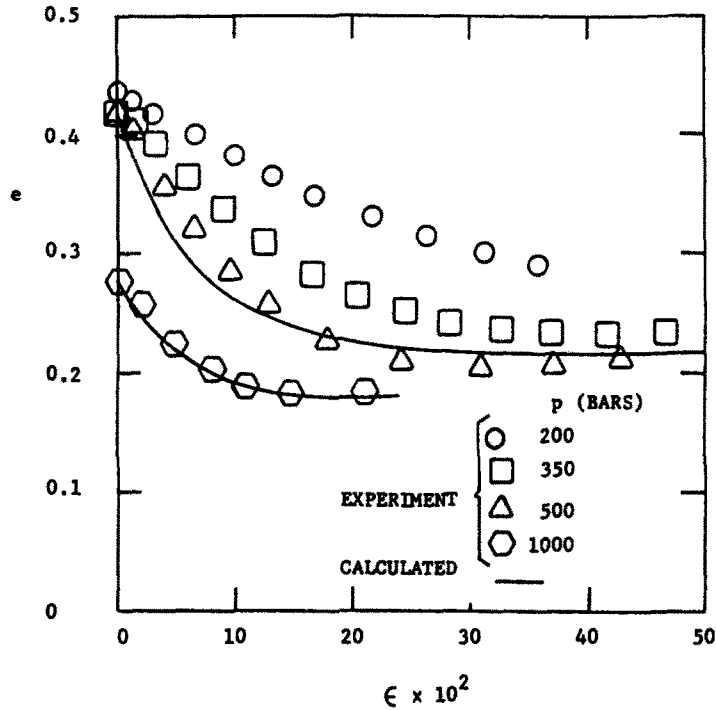
Fig. 11. Void ratio, e, vs the strain ϵ in triaxial tests of Ottawa sand; Experimental data from Zoback and Byerlee[10]; The theoretical (solid) curves display eqn (4.33): the upper solid curve corresponds to the q/p, ϵ-relation of Fig. 10, and the other curve to that of Fig. 9.

ing precursory events. In light of studies of this kind, we suggest that our constitutive relation has potentiality for quantitative application to problems of this kind. In particular, it is not difficult to explain stable fault movements in terms of gauge behavior similar to Curve (1) of Fig. 4(b). However, for unstable ruptures under very large confining pressures, the present model may predict large stress drops (if $\hat{h}/a$ in Fig. 4 is finite) which do not seem to occur during earthquakes. On the other hand, if $\hat{h}/a$ in Fig. 4 is small, or if the mechanism of rupture involves only a reduction in the frictional resistance (e.g. M being reduced by a certain amount), then the present model can be used to explain unstable fault movements and subsequent arresting processes. These and related matters will be carefully examined in a future report.

REFERENCES

1. C. A. Berg, Plastic dilation and void interaction. In *Inelastic Behavior of Solids* (Edited by M. F. Kanninen *et al.*), pp. 171–209. McGraw-Hill, New York (1970).
2. J. W. Rudnicki and J. R. Rice, Conditions for the localization of deformation in pressure-sensitive dilatant materials. *J. Mech. Phys. Solids* **23**, 371–394 (1975).
3. P. Wilde, Two invariant-dependent models of granular media. *Arc. Mech.* **29**, 799–809 (1977).
4. A. Schofield and P. Wroth, *Critical State Soil Mechanics.* McGraw-Hill, London (1968).
5. R. Hill, *The Mathematical Theory of Plasticity.* Oxford University Press (1950).
6. R. Hill, A general theory of uniqueness and stability in elastic-plastic solids. *J. Mech. Phys. Solid* **6**, 236–249 (1958).
7. S. Nemat-Nasser, Decomposition of strain measures and their rates in finite deformation elastoplasticity. *Int. J. Solids Structures* **15**, 155–166 (1979).
8. M. M. Mehrabadi and S. C. Cowin, Initial planar deformation of dilatant granular materials. *J. Mech. Phys. Solids* **26**, 269–284 (1978).
9. M. D. Zoback and J. D. Byerlee, A note on the deformational behavior and permeability of crushed granite. *Int. J. Rock Mech. Min. Sci & Geomech. Abstr.* **13**, 291–294 (1976).

10. M. D. Zoback and J. D. Byerlee, Effect of high-pressure deformation on permeability of Ottawa sand. *Bull. Am. Assoc. Petro. Geolog.* **60**, 1531–1542 (1976).
11. J. D. Byerlee, Brittle-ductile transition in rocks. *J. Geophys. Res.* **73**, 4741–4750 (1968).
12. J. D. Byerlee, The fracture strength and frictional strength of Weber sandstone. *Int. J. Rock Mech. Min Sci. & Geomech. Abstr.* **12**, 1–4 (1975).
13. J. R. Rice, Theory of precursory processes in the inception of earthquake rupture. *Proc. Symp. Phys. Earthquake Sources*, Academy of Sciences, German Democratic Republic, in press.
14. W. D. Stuart, Review of theories for earthquake instability. *Proc. Conf. III, Fault Mechs and its Relation to Earthquake Prediction* (Edited by J. F. Evernden), U.S. Geological Survey Open-File Report 78-380, Menlo Park, California, pp. 541–588 (1978).
15. W. D. Stuart, Diffusionless dilatancy model for earthquake precursors. *Geophys. Res. Lett.* **1**, 261–264 (1974).